



## Methane Gas Sensor using Graphene Nanoflakes at Room Operating Temperature

Siti Amaniah Mohd Chachuli<sup>1,\*</sup>, M. Aliff Ikhwan Che Azman<sup>1</sup>, Omer Coban<sup>2</sup>, Nur Hazahsha Shamsudin<sup>3</sup>

<sup>1</sup> Fakulti Teknologi dan Kejuruteraan Elektronik dan Komputer, Universiti Teknikal Malaysia Melaka (UTeM), Jalan Hang Tuah Jaya, 76100 Durian Tunggal, Melaka, Malaysia

<sup>2</sup> Faculty of Engineering, Ataturk University, Erzurum, Turkey

<sup>3</sup> Fakulti Teknologi dan Kejuruteraan Elektrik, Universiti Teknikal Malaysia Melaka (UTeM), Jalan Hang Tuah Jaya, 76100 Durian Tunggal, Melaka, Malaysia

### ARTICLE INFO

#### Article history:

Received 26 July 2024

Received in revised form 1 September 2024

Accepted 16 October 2024

Available online 30 November 2024

#### Keywords:

Methane; gas sensor; graphene nanoflakes; Kapton film; screen printing; organic binder

### ABSTRACT

Methane gas is commonly produced and used in various industries, including agriculture, coal mining, manure management, landfills, natural gas, and petroleum systems. This gas is colorless and odorless. High concentrations of methane gas can have detrimental effects on human health, such as causing headaches, visual issues, and memory loss. Moreover, prolonged exposure to higher concentrations may lead to respiratory and heart rate fluctuations, balance problems, and even unconsciousness. In order to address these concerns, a thick film gas sensor based on graphene nanoflakes is proposed in this work to detect different levels of methane gas at room operating temperature. The gas sensor was fabricated using screen-printing technology on a Kapton film. Graphene nanoflakes were mixed with a binder to create the sensing film. Scanning electron microscopy (SEM) was used to characterize the morphology and X-ray diffraction (XRD) for structural components of the sensing film. Two graphene gas sensors (PF-1 and PF-2) were fabricated using screen-printing to compare their performance to methane at room operating temperature with gas concentrations ranging from 300 to 1000 ppm. The results showed that both gas sensors responded robustly to changing concentrations of methane gas at room operating temperature within 20 s. PF-2 outperforms PF-1, with the result of sensitivity being approximately 0.0000353, 0.0000288, and 0.0000262 for the first, second, and third exposures to methane gas. Both gas sensors also exhibited excellent repeatability characteristics with similar patterns each time exposed to the methane.

## 1. Introduction

Methane is the most basic form of hydrocarbon, where it is made up of one carbon atom bonded to four hydrogen atoms. It is a highly combustible and explosive gas with no identifiable odor or color. It is not just a fuel, but it is also a harmful greenhouse gas that is about 24 times more powerful than

\* Corresponding author.

E-mail address: [sitiamaniah@utem.edu.my](mailto:sitiamaniah@utem.edu.my)

<https://doi.org/10.37934/armne.26.1.4453>

carbon dioxide at positive radiative forcing [1]. As a result, it is a significant contributor to global warming and it also has a very short lifespan in the atmosphere under normal conditions. On the other hand, because methane is such a powerful greenhouse gas, any considerable increase in its concentration in the atmosphere would almost certainly have disastrous implications. Environmental scientists are increasingly agreeing that methane is a more substantial contribution to global warming than carbon dioxide. As a result, the damage is rapid and irreparable. When the quantity of methane in the air with the concentration range is 5-14%, there is a risk of explosion [2]. On the other hand, methane has the potential to trigger an explosion. Methane is, however, extremely difficult to detect due to the non-polarity and high enthalpy of the C-H bond [1]. This is incontrovertible proof that we require the development of a technology for detecting methane that is accessible, quick, efficient, and dependable in order to provide early warning and ensure the protection of both life and property.

Nowadays, sensors are the key means of obtaining varied information in modern measurement, automation control, safety monitoring, environmental monitoring, and medical and military areas. Hazardous gases such as methane need to detect and identify this type of gas. Various types of gas sensors have been proposed by researchers, such as fiber optic [3] and semiconductor sensors [4-7]. A chemical-based gas sensor is an analysis that selectively and permanently responds to a given analyte and translates input chemical amounts into an electrical signal, such as the concentration of a single sample component or a complete composition analysis [8]. Various types of sensing materials examined by researchers to sense methane include tin dioxide ( $\text{SnO}_2$ ) [1,4-7], indium oxide ( $\text{In}_2\text{O}_3$ ) [8,9], titanium dioxide ( $\text{TiO}_2$ ) [10], tungsten oxide ( $\text{WO}_3$ ) [11], multi-walled carbon nanotube (MWCNT) [2], and cobalt chromite ( $\text{CoCr}_2\text{O}_4$ ) [12],  $\text{LaFeO}_3$  [13], and graphene oxide (GO) [14].

However, metal oxide needs to work at high operating temperatures up to  $350^\circ\text{C}$  [6,8] in order to sense the graphene, which can also cause high power consumption. Therefore, a metal-based gas sensor based on graphene is proposed in this study to ensure that methane can be detected at room operating temperature. Graphene has a high surface area, low resistivity, and high carrier mobility [13], and was chosen as the sensing material in this work. A similar graphene gas sensor in a prior study has been reported to have the ability to detect acetone and nitrogen oxide gas at room operating temperature [15]. A study in [15] presented graphene nanoflakes as a promising material in gas sensors since reactivity and sensitivity have been improved toward molecular adsorption and showed a response to nitrogen oxide. Other than that, graphene nanoflakes also have been applied in many studies such as lithium-ion batteries [16], the toxic effect [17],  $\text{CO}_2$ -assisted oxidative dehydrogenation of propane [18], counter electrode in dye-sensitized solar cells [19], hydrazine-sensing [20], saturable absorber [21], antibacterial study [22], and determination of citrinin in food [23]. With the excellent properties of graphene, a high response methane gas sensor is expected to be produced in this study.

The goal of this endeavor is to adopt a simple and effective method to develop a graphene nanoflakes-based gas sensor using a screen-printing technique that can be used as a flexible gas sensor by using a Kapton film as a substrate. Two similar graphene gas sensors were fabricated and exposed to the methane to compare their characteristics. The results demonstrated that the graphene gas sensor is responsive, has great repeatability, and is sensitive to 300-1000 ppm of methane at room operating temperature.

## 2. Methodology

### 2.1 Preparation of Graphene Nanoflakes Paste

The sensing layer for the graphene gas sensor is prepared in two major steps: preparation of the binder and preparation of the graphene nanoflakes paste. Ethyl cellulose and  $\alpha$ -terpineol were employed in this work as the organic binder. To create a homogeneous binder for sensing material, 95 wt.% of  $\alpha$ -terpineol and 5 wt.% of ethyl cellulose were mixed together using a magnetic stirrer. Figure 1 shows the process of preparation of the binder. This mixing took place for eight hours at 250 revolutions per minute (rpm) and 40°C temperature. Furthermore, for the sensing layer of the gas sensor, 94 wt.% of binder was combined with 6 wt.% of graphene nanoflakes for at least 8 hours while being magnetically swirled until a homogenous and viscous paste was obtained as depicted in Figure 2. The preparation of graphene nanoflakes paste in this work was adapted from method presented in [24].

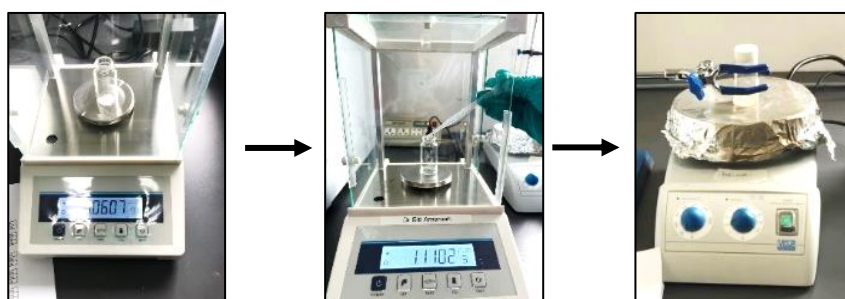


Fig. 1. Process preparation of binder

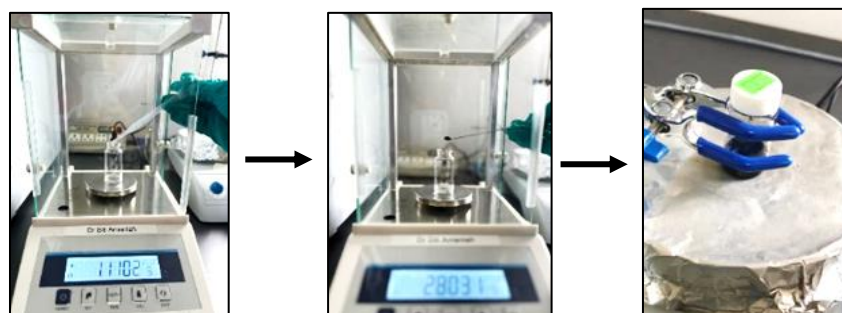
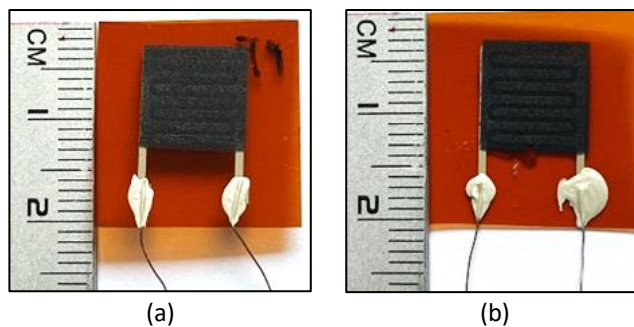


Fig. 2. Process preparation of graphene nanoflakes paste

### 2.2 Fabrication of Graphene Nanoflakes Gas Sensor Using Screen-Printing Technology

A Kapton film was chosen as a substrate of the gas sensor and was cut into 2.0 cm X 2.0 cm squares. To ensure the Kapton films were spotless, isopropyl alcohol was wiped onto the surface of the Kapton film. The graphene nanoflakes gas sensor consists of two layers: an interdigitated electrode and a sensing layer. Firstly, an interdigitated electrode was printed onto a substrate using a screen-printing technique using a silver paste and followed by 15 minutes of annealing at 150°C using an oven. Graphene nanoflake paste is layered atop an interdigitated electrode as sensing material of the gas sensor with a size of 1 cm x 1 cm and annealed at 200°C for 30 minutes in the oven. After the deposition of sensing material and the interdigitated electrode on Kapton film have been completed, fine copper wires of about 2.5 cm in length are utilized in both of these processes to create an electrical connection. The fabrication technique of the gas sensor was adapted from [24]. Two similar graphene nanoflakes gas sensors were fabricated to compare both performances to the methane, as displayed in Figure 3 and labeled as PF-1 and PF-2.



**Fig. 3.** Fabricated graphene gas sensor using a screen-printing technique (a) PF-1 (b) PF-2

### 2.3 Current Measurement of Graphene Nanoflakes Gas Sensor

The experimental setup for the measurement of the gas sensor to the methane is depicted in Figure 4. The computer, the mass flow module (MFM), and the source metre (Keithley 6482) are all linked to the gas chamber through their respective cables. The MFM will control the flow of gas through the sensor. The LabVIEW software was utilized to monitor the changes that occurred in the output (current). The gas sensor is placed inside the gas chamber along with the current measurement process. Initially, nitrogen acts as carrier gas and will flow to the gas sensor in 5 minutes for stabilization. After obtaining a stable current, the methane gas was exposed to the gas sensor in the gas chamber for 10 minutes to determine the response time. After being exposed to methane gas for 10 minutes, the nitrogen gas will be exposed for 15 minutes, at which point the recovery time will be determined.

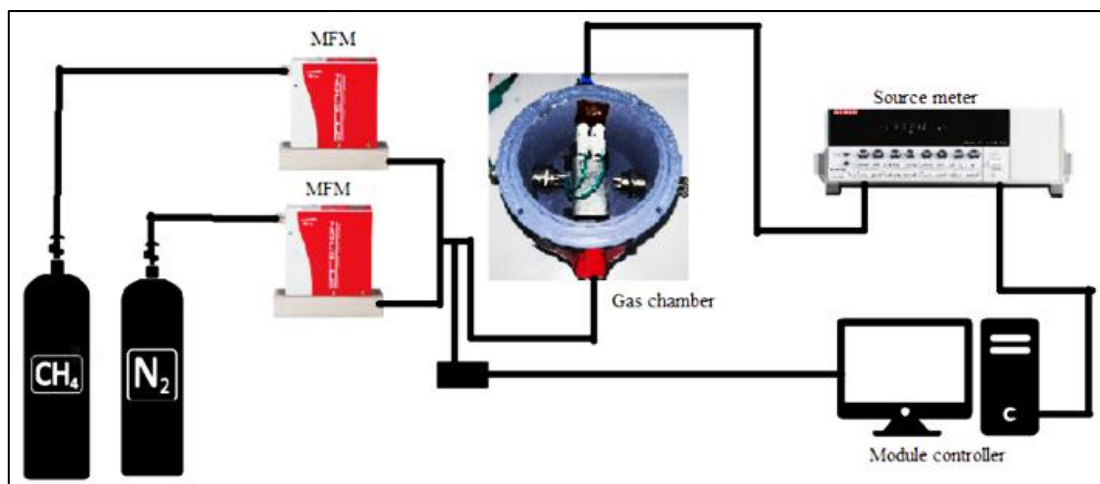


**Fig. 4.** Experimental setup of gas sensor to the methane

## 3. Results

### 3.1 Characterization of Sensing Layer using Scanning Electron Microscope (SEM) and X-ray diffraction (XRD)

SEM and XRD characterizations of the surface of the gas sensor on the Kapton film after annealing at 200°C are presented in Figure 5. It can be seen that the morphology of the graphene was flakes, which confirmed that the sensing material on the surface of the gas sensor after annealing treatment was graphene flakes. The flake structure was also similar, as observed in [17,25]. The flakes were measured using JImage software, and it was found that the flake's diameters ranged from 10 to 30

$\mu\text{m}$ . The cross-section of the sensing layer was conducted by cutting the sensing layer at the center. It can be observed that the sensing layer was uneven because the size of the flakes was not identical. The height of the flakes was approximately in the range of 10-20  $\mu\text{m}$ .

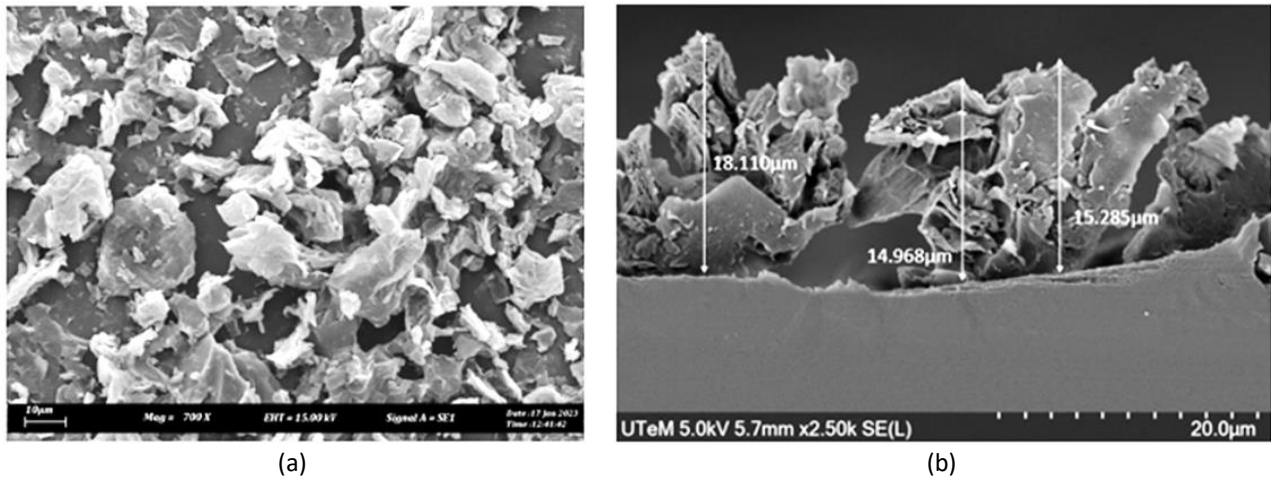


**Fig. 5.** Characterization of the gas sensor surface using SEM (a) Morphology (b) Cross-section

Figure 6 shows XRD spectra of the sensing layer after annealing treatment. It can be seen that there is one single broad peak was detected in XRD spectra at  $2\theta=18.43^\circ$ . As reported in [23-25], the single broad peak that occurred at  $2\theta=26^\circ$  belonged to graphene. However, the peak detected in Figure 6 occurred at  $2\theta=18.43^\circ$ , where this peak has been shifted. This phenomenon might be caused by the mixing and annealing process. According to [26-28], the peak for graphene oxide occurred at  $11.1^\circ$  thus, this study suggests that some of the elements in graphene nanoflakes also have been changed to graphene oxide after being annealed in ambient air. This behaviour might occur because a large amount of ionized oxygen was bound to the graphene during the annealing process, resulting in the graphene oxide feature. Besides that, the mixing of graphene nanoflakes and binder also might contribute to the changes in the graphene nanoflakes structures.

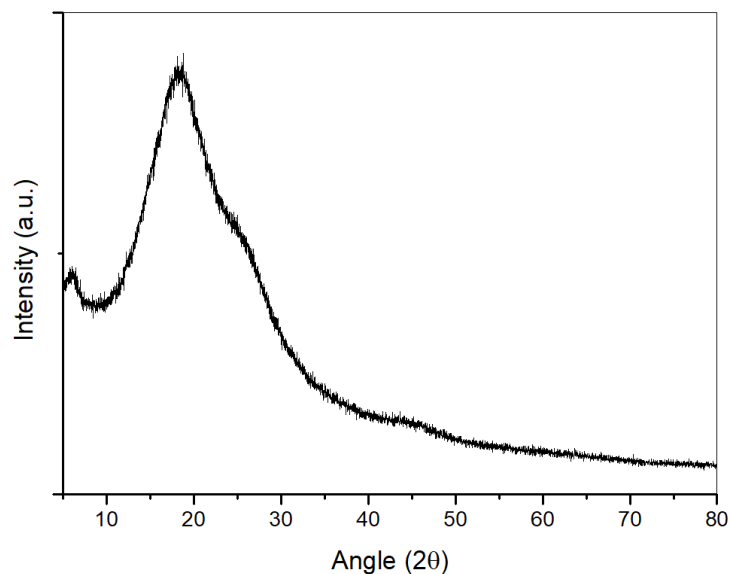


**Fig. 6.** XRD spectra for sensing layer with annealing treatment

### 3.2 Current-Voltage (I-V) Characteristic of Graphene Nanoflakes Gas Sensor

The graphene gas sensor's current-voltage (I-V) characteristic was carried out using a two-point probe method using a source meter (Keithley 6482). LabVIEW software was used to set the supply voltage and monitor the output current of the gas sensor. Figure 7 shows the I-V characteristic of the fabricated gas sensor at a voltage source from -1V to 1V. The resistance of the fabricated gas sensor was calculated by applying Ohm's law to check the linearity. The resistance value of the graphene gas sensor is 2.073 kΩ for PF-1 and 1.669 kΩ for PF-2. Both gas sensors produced linear characteristics, following Ohm's law and permitting the exposing of the gas sensors to methane. These linear characteristics indicate that good ohmic contacts are formed between the sensing layer and electrodes [29].

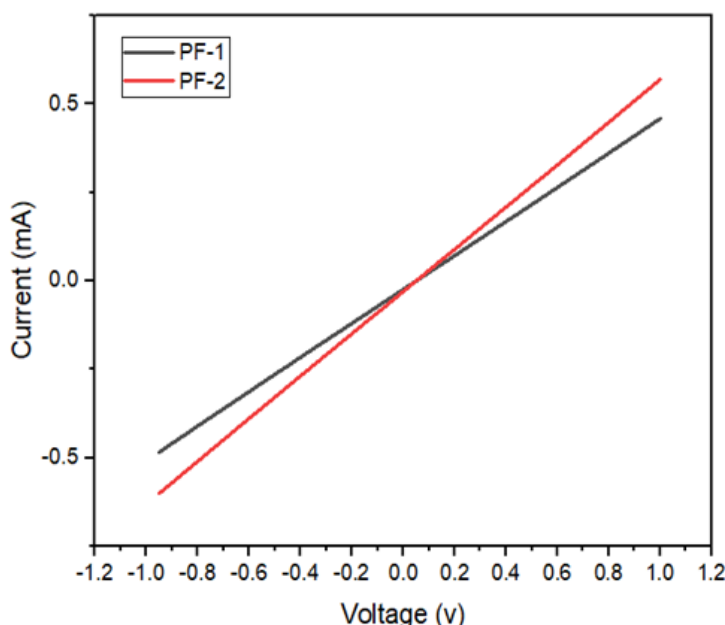


Fig. 7. Current-voltage of graphene gas sensor at -1V to 1V

### 3.3 Characteristics of Graphene Nanoflakes Gas Sensor to Methane

Figure 8 shows the current measurement and sensitivity of graphene nanoflakes gas sensors to various concentrations of methane in the range of 300-1000 ppm. The characteristics of the gas sensor were evaluated in terms of response, sensitivity, and repeatability properties. The response of the graphene gas sensor was evaluated using the formula as follows:

$$Response = \frac{I_g}{I_n} \quad (1)$$

where  $I_g$  is current during methane flow, and  $I_g$  value is taken at the maximum value of current during methane exposure, while  $I_n$  is current during nitrogen flow and  $I_n$  value is taken at a stable value during nitrogen exposure. A repeatability test was conducted by exposing both gas sensors to 300-1000 ppm of methane three times to observe the methane sensing pattern. The sensitivity value was calculated by finding the slope of the response graph for 300-1000 ppm of methane.

The result indicated that both gas sensors responded to the methane as n-typed gas sensors, with increased current when exposed to the reducing gas (methane) and decreased current when exposed to the carrier gas (nitrogen), as shown in Figure 9. This result also verified that the graphene



nanoflakes used in this study are n-typed semiconductors based on the sensor response. The gas sensor was exposed to 300-1000 ppm of methane three times to study the repeatability properties. It can be observed that PF-1 and PF-2 showed a similar pattern to the methane. It also revealed that the current was increased when the gas sensor was exposed for a second time and increased again when exposed to the methane a third time. The sensitivity values for the PF-1 gas sensor were approximately  $2.91 \times 10^{-5}$ ,  $1.68 \times 10^{-5}$ , and  $1.82 \times 10^{-5}$ , respectively. Whereas sensitivity values for the PF-2 gas sensor were approximately  $3.53 \times 10^{-5}$ ,  $2.88 \times 10^{-5}$ , and  $2.62 \times 10^{-5}$ , respectively. Both gas sensors (PF-1 and PF-2) produced the highest sensitivity for the first time exposed to methane. It can be seen that the sensitivity was reduced when exposed for the second time and third time.

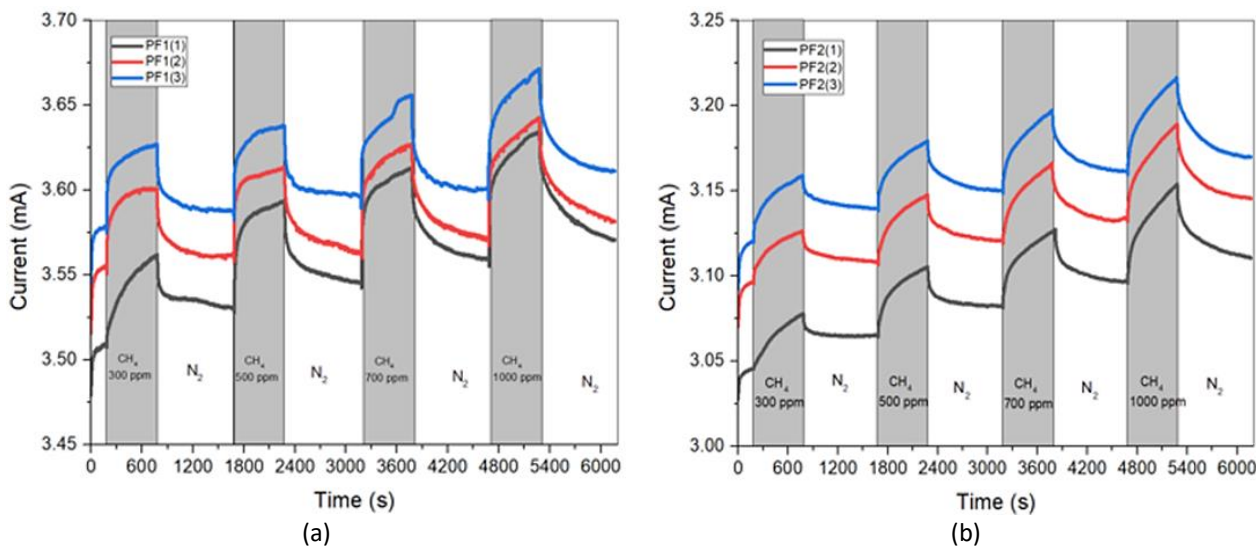


Fig. 8. Current measurement of graphene nanoflakes gas sensor to methane (a) PF-1 (b) PF-2

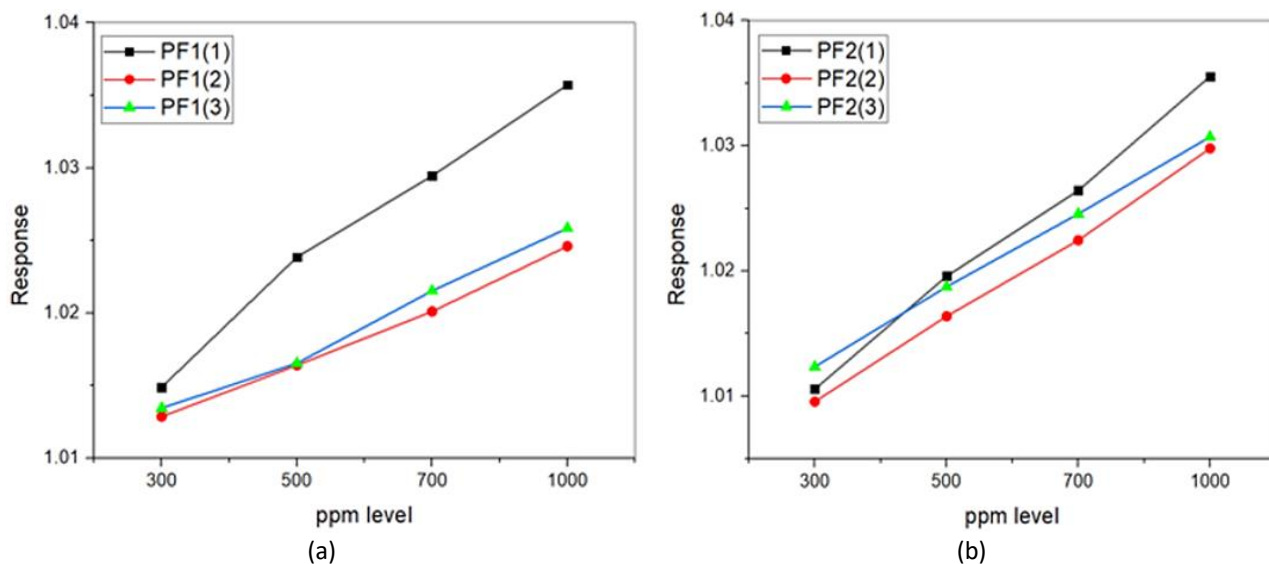


Fig. 9. Response of graphene nanoflakes gas sensor to methane (a) PF-1 (b) PF-2

Table 1 lists the response value, response time, and recovery time for PF-1 and PF-2 gas sensors to the 300-1000 ppm of methane. It can be seen that the response value varies in the range of 1.0106-1.0357. The fastest response time was recorded at 220 s for 300 ppm, while the fastest recovery time was recorded at 193 s for 500 ppm. It also can be observed that the response values were increased when the methane concentrations also increased. All the gas sensors showed a quick change when

exposed to the methane, which is less than 20 s, as seen in Figure 8, where this phenomenon supports that the graphene gas sensor in this work is responsive to methane. Meanwhile, both gas sensors also reached 90% from the maximum value was less than 500 s, which suggests graphene nanoflakes responsive to the methane at room operating temperature. The measurement of methane response also did not use a vacuum gas to flow the methane gas to the gas sensor; this indicated that the fabricated methane gas sensor is a good sensor, where the current of the gas sensor can respond in a faster time and recover itself without the help of the vacuum. With this feature, the methane gas sensor can be applied in any application.

**Table 1**

Response time and recovery time of the gas sensors to the methane

Sample	Concentration (ppm)	Response			Response time (s)			Recovery time (s)		
		1	2	3	1	2	3	1	2	3
PF1	300	1.0149	1.0129	1.0135	444	220	322	604	604	258
	500	1.0239	1.0164	1.0165	269	289	248	446	446	301
	700	1.0295	1.0201	1.0215	322	310	410	469	469	238
	1000	1.0357	1.0246	1.0258	376	421	417	408	408	430
PF2	300	1.0106	1.0096	1.0124	453	429	460	166	466	447
	500	1.0196	1.0164	1.0187	431	443	455	253	440	193
	700	1.0264	1.0225	1.0246	467	468	466	438	319	437
	1000	1.0355	1.0298	1.0307	475	479	462	529	466	487

#### 4. Conclusions

The graphene nanoflakes gas sensor was successfully fabricated using screen-printing. The gas sensor exhibited a good response to methane. Furthermore, the fabricated graphene gas sensor also showed excellent response time, recovery time, sensitivity and repeatability properties to the methane. In conclusion, in terms of sensitivity, PF-2 outperforms PF-1. For the first, second, and third exposures to methane gas, PF-2 has 3.53E-05, 2.088E-05, and 2.62E-05, respectively. The responsiveness, response time, and recovery time parameters of PF-1 and PF-2 are nearly identical.

#### Acknowledgement

We would like to express our gratitude to the Universiti Teknikal Malaysia Melaka (UTeM) for sponsoring this project under short term grant with grant no: PJP/2021/FKEKK/S01821.

#### References

- [1] Yao, Lijia, Yuxiu Li, Yan Ran, Yue Yang, Rongjun Zhao, Linfeng Su, Yulin Kong, Dian Ma, Yunhua Chen, and Yude Wang. "Construction of novel Pd-SnO<sub>2</sub> composite nanoporous structure as a high-response sensor for methane gas." *Journal of Alloys and Compounds* 826 (2020): 154063. <https://doi.org/10.1016/j.jallcom.2020.154063>
- [2] Shukla, Prashant, Pooja Saxena, Devinder Madhwal, Nitin Bhardwaj, and V. K. Jain. "Electrostatically functionalized CVD grown multiwalled carbon nanotube/palladium polymer nanocomposite (MWCNT/Pd) for methane detection at room temperature." *Chemical Engineering Science* 264 (2022): 118191. <https://doi.org/10.1016/j.ces.2022.118191>
- [3] Fu, Haiwei, Xiaoling Wang, Jijun Ding, Xingyu Yan, Ziliang Zhao, and Ze Zhang. "SnO<sub>2</sub>/Graphene incorporated optical fiber Mach-Zehnder interferometer for methane gas detection." *Optical Fiber Technology* 74 (2022): 103126. <https://doi.org/10.1016/j.yofte.2022.103126>
- [4] Yang, Boxuan, Zheng Zhang, Chen Tian, Wenjing Yuan, Zhongqiu Hua, Shurui Fan, Yi Wu, and Xuemin Tian. "Selective detection of methane by HZSM-5 zeolite/Pd-SnO<sub>2</sub> gas sensors." *Sensors and Actuators B: Chemical* 321 (2020): 128567. <https://doi.org/10.1016/j.snb.2020.128567>
- [5] Moalaghi, Maryam, Mohsen Ghareji, Alireza Ranjkesh, and Faramarz Hossein-Babaei. "Tin oxide gas sensor on tin oxide microheater for high-temperature methane sensing." *Materials Letters* 263 (2020): 127196. <https://doi.org/10.1016/j.matlet.2019.127196>



- [6] Wu, Ruijie, Liang Tian, Hao Li, Huabin Liu, Jiabin Luo, Xuemin Tian, Zhongqiu Hua, Yi Wu, and Shurui Fan. "A selective methane gas sensor based on metal oxide semiconductor equipped with an on-chip microfilter." *Sensors and Actuators B: Chemical* 359 (2022): 131557. <https://doi.org/10.1016/j.snb.2022.131557>
- [7] Li, Juan, Yilun Ma, Zaihua Duan, Yajie Zhang, Xiaohui Duan, Bohao Liu, Zhen Yuan, Yuanming Wu, Yadong Jiang, and Huiling Tai. "Local dynamic neural network for quantitative analysis of mixed gases." *Sensors and Actuators B: Chemical* 404 (2024): 135230. <https://doi.org/10.1016/j.snb.2023.135230>
- [8] Kgomo, M. B., K. Shingange, M. I. Nemifulwi, Hendrik C. Swart, and Gugu Hlengiwe Mhlongo. "Belt-like In<sub>2</sub>O<sub>3</sub> based sensor for methane detection: Influence of morphological, surface defects and textural behavior." *Materials Research Bulletin* 158 (2023): 112076. <https://doi.org/10.1016/j.materresbull.2022.112076>
- [9] Lu, Ning, Shurui Fan, Yaxu Zhao, Boxuan Yang, Zhongqiu Hua, and Yi Wu. "A selective methane gas sensor with printed catalytic films as active filters." *Sensors and Actuators B: Chemical* 347 (2021): 130603. <https://doi.org/10.1016/j.snb.2021.130603>
- [10] Arafat, M. M., A. S. M. A. Haseeb, S. A. Akbar, and Md Zakaria Quadir. "In-situ fabricated gas sensors based on one dimensional core-shell TiO<sub>2</sub>-Al<sub>2</sub>O<sub>3</sub> nanostructures." *Sensors and Actuators B: Chemical* 238 (2017): 972-984. <https://doi.org/10.1016/j.snb.2016.07.135>
- [11] Yu, J., Hao Wen, Mahnaz Shafiei, M. R. Field, Z. F. Liu, Wojtek Wlodarski, Nunzio Motta, Y. X. Li, Kourosh Kalantar-zadeh, and P. T. Lai. "A hydrogen/methane sensor based on niobium tungsten oxide nanorods synthesised by hydrothermal method." *Sensors and Actuators B: Chemical* 184 (2013): 118-129. <https://doi.org/10.1016/j.snb.2013.03.135>
- [12] Pasha, Apsar, Mohd Ubaidullah, Manish Gupta, Bidhan Pandit, S. O. Manjunatha, and Satbir S. Sehgal. "Rare earth (Sm<sup>3+</sup>) doped CoCr<sub>2</sub>O<sub>4</sub> ceramics sensor towards room temperature detection of greenhouse methane gas." *Ceramics International* 49, no. 10 (2023): 16174-16181. <https://doi.org/10.1016/j.ceramint.2023.01.215>
- [13] Duan, Xiaohui, Yadong Jiang, Bohao Liu, Zaihua Duan, Yajie Zhang, Zhen Yuan, and Huiling Tai. "Enhancing the carbon dioxide sensing performance of LaFeO<sub>3</sub> by Co doping." *Sensors and Actuators B: Chemical* 402 (2024): 135136. <https://doi.org/10.1016/j.snb.2023.135136>
- [14] Assar, Mohammadreza, and Rouhollah Karimzadeh. "Enhancement of methane gas sensing characteristics of graphene oxide sensor by heat treatment and laser irradiation." *Journal of colloid and interface science* 483 (2016): 275-280. <https://doi.org/10.1016/j.jcis.2016.08.045>
- [15] Mohd Chachuli, Siti Amaniah, Yap Pei Yeuan, Omer Coban, NH Shamsudin, and M. Idzihar IDRIS. "Investigation of Graphene Gas Sensor at Different Substrates for Acetone Detection." *Przegląd Elektrotechniczny* 99, no. 3 (2023). <https://doi.org/10.15199/48.2023.03.51>
- [16] Stolbov, Dmitrii, Sergei Chernyak, Anton Ivanov, Konstantin Maslakov, Evgeniya Tveritina, Vitaly Ordonsky, Mingzhu Ni, Serguei Savilov, and Hui Xia. "Silicon-doped graphene nanoflakes with tunable structure: Flexible pyrolytic synthesis and application for lithium-ion batteries." *Applied Surface Science* 592 (2022): 153268. <https://doi.org/10.1016/j.apsusc.2022.153268>
- [17] Urban-Malinga, Barbara, Magdalena Jakubowska, Anna Hallmann, and Agnieszka Dąbrowska. "Do the graphene nanoflakes pose a potential threat to the polychaete Hediste diversicolor?." *Chemosphere* 269 (2021): 128685. <https://doi.org/10.1016/j.chemosphere.2020.128685>
- [18] Chernyak, Sergei A., Alexander L. Kustov, Dmitrii N. Stolbov, Marina A. Tedeeva, Oksana Ya Isaikina, Konstantin I. Maslakov, Nadezhda V. Usol'tseva, and Serguei V. Savilov. "Chromium catalysts supported on carbon nanotubes and graphene nanoflakes for CO<sub>2</sub>-assisted oxidative dehydrogenation of propane." *Applied Surface Science* 578 (2022): 152099. <https://doi.org/10.1016/j.apsusc.2021.152099>
- [19] Wu, Wen-Tuan, Shun-Han Yang, Ching-Ming Hsu, and Wen-Ti Wu. "Study of graphene nanoflake as counter electrode in dye sensitized solar cells." *Diamond and Related Materials* 65 (2016): 91-95. <https://doi.org/10.1016/j.diamond.2016.02.022>
- [20] Mutyala, Sankararao, and Jayaraman Mathiyarasu. "Preparation of graphene nanoflakes and its application for detection of hydrazine." *Sensors and Actuators B: Chemical* 210 (2015): 692-699. <https://doi.org/10.1016/j.snb.2015.01.033>
- [21] Rashid, Nur Nadhirah Mohamad, Hariith Ahmad, Mohammad Faizal Ismail, Siti Nur Fatin Zuikafly, Nur Azmah Nordin, Tsuyoshi Koga, Wira Jazair Yahya, Hafizal Yahaya, and Fauzan Ahmad. "Passively Q-switched thulium-holmium doped fibre laser with electrochemical exfoliation graphene in chitin based passive saturable absorber." *Journal of Advanced Research in Micro and Nano Engineering* 11, no. 1 (2023): 1-14. <https://doi.org/10.37934/armne.11.1.114>
- [22] Ismail, Nur'Afini, Kamyar Shameli, Roshafima Rasit Ali, Siti Nur Amalina Mohamad Sukri, and Eleen Dayana Mohamed Isa. "Copper/graphene based materials nanocomposites and their antibacterial study: A mini review." *Journal of Research in Nanoscience and Nanotechnology* 1, no. 1 (2021): 44-52. <https://doi.org/10.37934/jrnn.1.1.4452>

- [23] Elfadil, Dounia, Filippo Silveri, Sara Palmieri, Flavio Della Pelle, Manuel Sergi, Michele Del Carlo, Aziz Amine, and Dario Compagnone. "Liquid-phase exfoliated 2D graphene nanoflakes electrochemical sensor coupled to molecularly imprinted polymers for the determination of citrinin in food." *Talanta* 253 (2023): 124010. <https://doi.org/10.1016/j.talanta.2022.124010>
- [24] Mohd Chachuli, Siti Amaniah, Mohd Nizar Hamidon, Mehmet Ertugrul, Md Shuhazlly Mamat, H. Jaafar, and Norhafiz Aris. "Influence of B<sub>2</sub>O<sub>3</sub> addition on the properties of TiO<sub>2</sub> thick film at various annealing temperatures for hydrogen sensing." *Journal of Electronic Materials* 49 (2020): 3340-3349. <https://doi.org/10.1007/s11664-020-08059-0>
- [25] Yu, Kui, Haitao Ma, Yanhua Guo, Zhonggang Sun, Yuecheng Dong, Igor V. Alexandrov, Egor A. Prokofiev, and Hui Chang. "Microstructure evolution and mechanical properties of copper coated graphene nanoflakes/pure titanium matrix composites." *Materials Characterization* 194 (2022): 112422. <https://doi.org/10.1016/j.matchar.2022.112422>
- [26] Kamal, Tahseen. "High performance NiO decorated graphene as a potential H<sub>2</sub> gas sensor." *Journal of Alloys and Compounds* 729 (2017): 1058-1063. <https://doi.org/10.1016/j.jallcom.2017.09.124>
- [27] Zhang, Dongzhi, Chuanxing Jiang, and Yong Zhang. "Room temperature hydrogen gas sensor based on palladium decorated tin oxide/molybdenum disulfide ternary hybrid via hydrothermal route." *Sensors and Actuators B: Chemical* 242 (2017): 15-24. <https://doi.org/10.1016/j.snb.2016.11.005>
- [28] Zaki, Shrouk E., Mohamed A. Basyooni, Mohamed Shaban, Mohamed Rabia, Yasin Ramazan Eker, Gamal F. Attia, Mucahit Yilmaz, and Ashour M. Ahmed. "Role of oxygen vacancies in vanadium oxide and oxygen functional groups in graphene oxide for room temperature CO<sub>2</sub> gas sensors." *Sensors and Actuators A: Physical* 294 (2019): 17-24. <https://doi.org/10.1016/j.sna.2019.04.037>
- [29] Zhang, Yong, Zaihua Duan, Hefeng Zou, and Mo Ma. "Fabrication of electrospun LaFeO<sub>3</sub> nanotubes via annealing technique for fast ethanol detection." *Materials Letters* 215 (2018): 58-61. <https://doi.org/10.1016/j.matlet.2017.12.062>